A Dual-Functional Rhodamine B and Azo-Salicylaldehyde Derivative for Simultaneous Detection of Copper and Hypochlorite: Synthesis, Biological Applications and Theoretical Insights

Vishnu S[a], Yatheesharadhya bylappa[b], Anish Nag[b], Malay Dolai[c] and Avijit Kumar Das[a]*

[a]Department of Chemistry, Christ University, Hosur Road, Bangalore, Karnataka, 560029 India,

*Email: avijitkumar.das@christuniversity.in

[b]Department of Life Science, Christ University, Hosur Road, Bangalore, Karnataka, India, 560029

[c]Department of Chemistry, Prabhat Kumar College, Contai, Purba Medinipur 721404, W.B., India.

CONTENTS

1. Experimental

1.1. General:

Unless otherwise mentioned, chemicals and solvents were purchased from Sigma-Aldrich chemicals Private Limited and were used without further purification. ^{1}H-NMR spectra were recorded on Brucker 400 MHz instrument. For NMR spectra, d^6-DMSO was used as solvent using TMS as an internal standard. Chemical shifts are expressed in δ- units and ^{1}H–^{1}H and ^{1}H–C coupling constants in Hz. UV-vis titration experiments were performed on a UV-Spectrophotometer: PerkinElmer, Lambda 30 and fluorescence experiment was done using Shimadzu RF-5301PC Fluorescence spectrofluorometer using a fluorescence cell of 10 mm path.

1.2. General method of UV-vis and fluorescence titration:

By UV-vis method:

For UV-vis titrations, stock solution of the sensor was prepared (c = 2 x 10^{-5} M) in CH_3CN-HEPES buffer (9/1, v/v, 25°C) at pH 7.4. The solution of the guest interfering analytes like Ni^{2+}, Mn^{2+}, Pb^{2+}, Cd^{2+}, Fe^{2+}, Cu^{2+}, Fe^{3+}, Zn^{2+}, Co^{2+}, Al^{3+}, Hg^{2+} as their chloride salts were also prepared in the order of c = 2x10^{-4}M. Solutions of various concentrations containing sensor and increasing concentrations of cations were prepared separately. The spectra of these solutions were recorded by means of UV-vis methods. For UV-vis titrations with ct-DNA and BSA, stock solution of the sensor was prepared (c = 2× 10^{-5} M) in DMSO- Tris-HCl buffer (40 µL in 2 ml Tris-HCl buffer) at pH 7.2. Tris-HCl buffer was used to prepare the solution of ct-DNA (2 mM in base pairs) and BSA (c = 7.4 µM). The spectra of these solutions were recorded by means of UV-vis methods.

General procedure for drawing Job plot by UV–vis method:

Stock solution of same concentration of **BBS** and Cu^{2+} were prepared in the order of ≈ 2.0 x 10^{-5} M in CH_3CN-HEPES buffer (9:1, v/v, pH = 7.4). The absorbance in each case with different *host–guest* ratio but equal in volume was recorded. Job plots were drawn by plotting $\Delta I.X_{host}$ *vs* X_{host} (ΔI = change of intensity of the absorbance spectrum during titration and X_{host} is the mole fraction of the host in each case, respectively).

By fluorescence method:

For fluorescence titrations, stock solution of the sensor (c = 2 x 10^{-5} M) was prepared for the titration of cations in CH_3CN-HEPES buffer [9:1, v/v, pH = 7.4]. The solution of the guest cations using their chloride salts in the order of 200 µM were also prepared. Solutions of various concentrations containing sensor and increasing concentrations of cations were

prepared separately. The spectra of these solutions were recorded by means of fluorescence methods. For UV-vis titrations with ct-DNA and BSA, stock solution of the sensor was prepared ($c = 2\times 10^{-5}$ M) in DMSO- Tris-HCl buffer (40 µL in 2 ml Tris-HCl buffer) at pH 7.2. Tris-HCl buffer was used to prepare the solution of ct-DNA (2 mM in base pairs) and BSA (c = 7.4 µM). The spectra of these solutions were recorded by means of UV-vis methods.

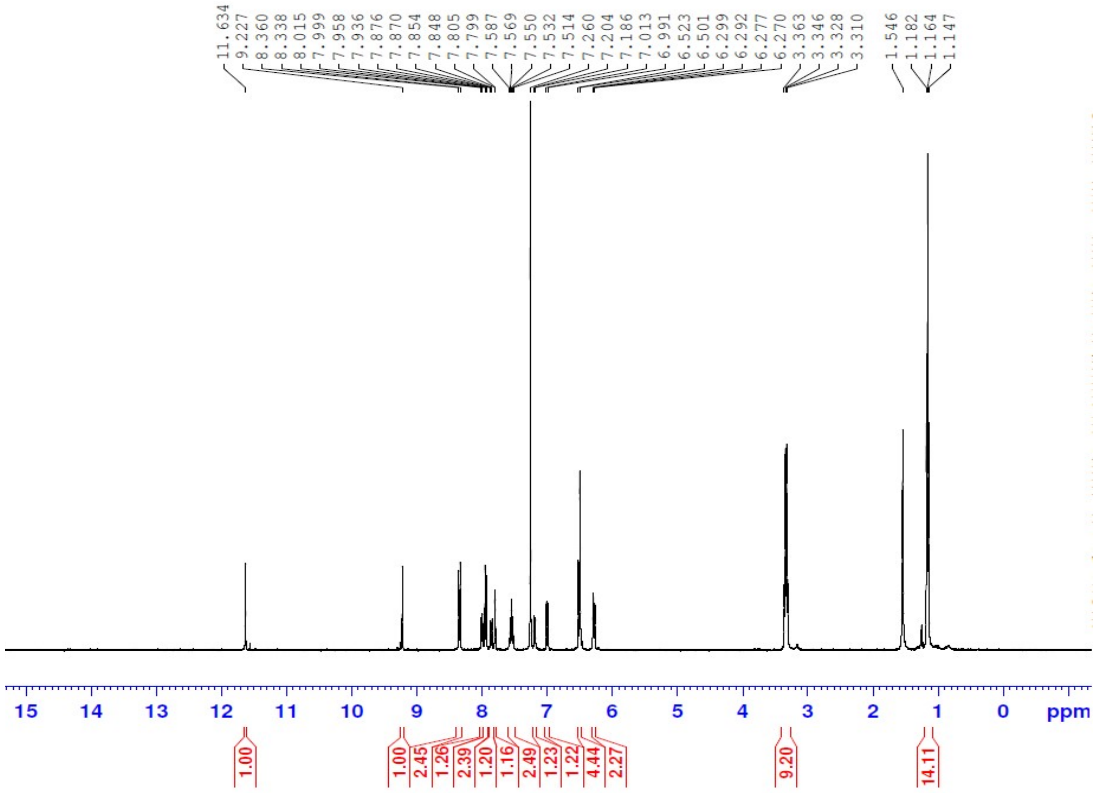

Figure S1. ^{1}H NMR spectrum of **BBS**

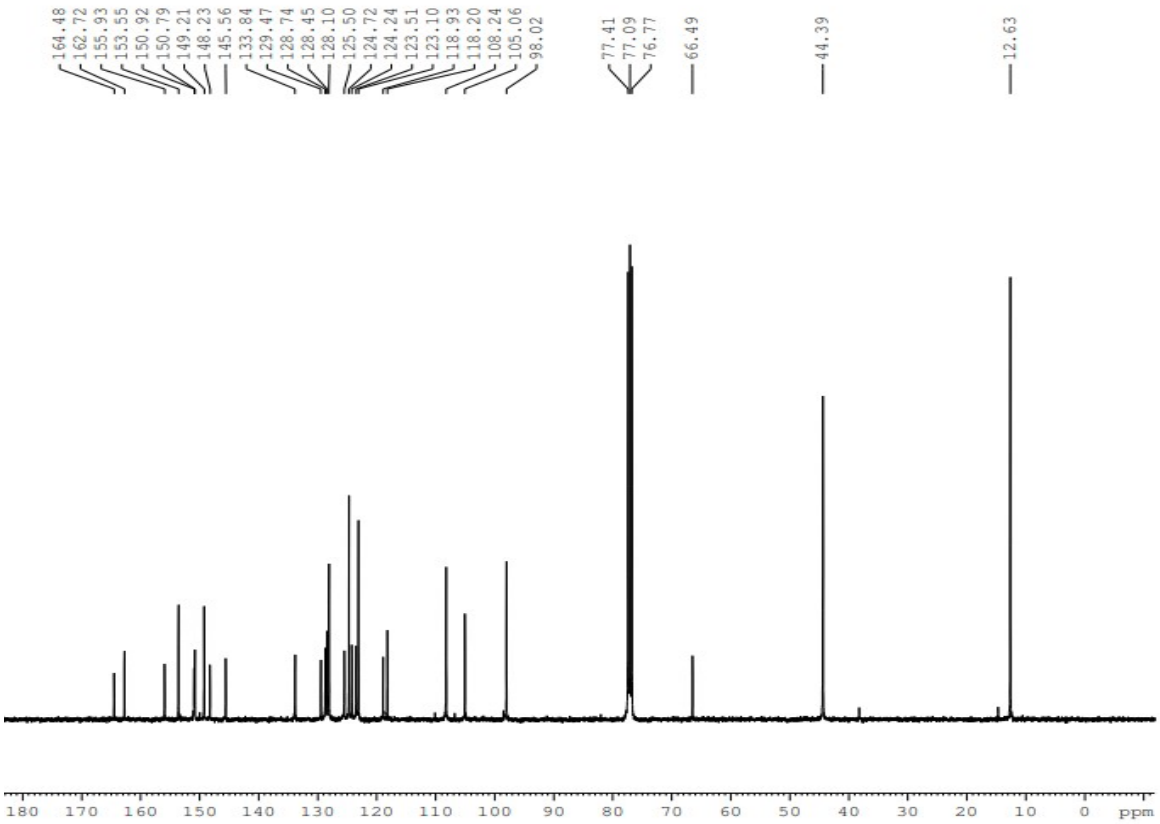

Figure S2. ^{1}H NMR spectrum of **BBS**

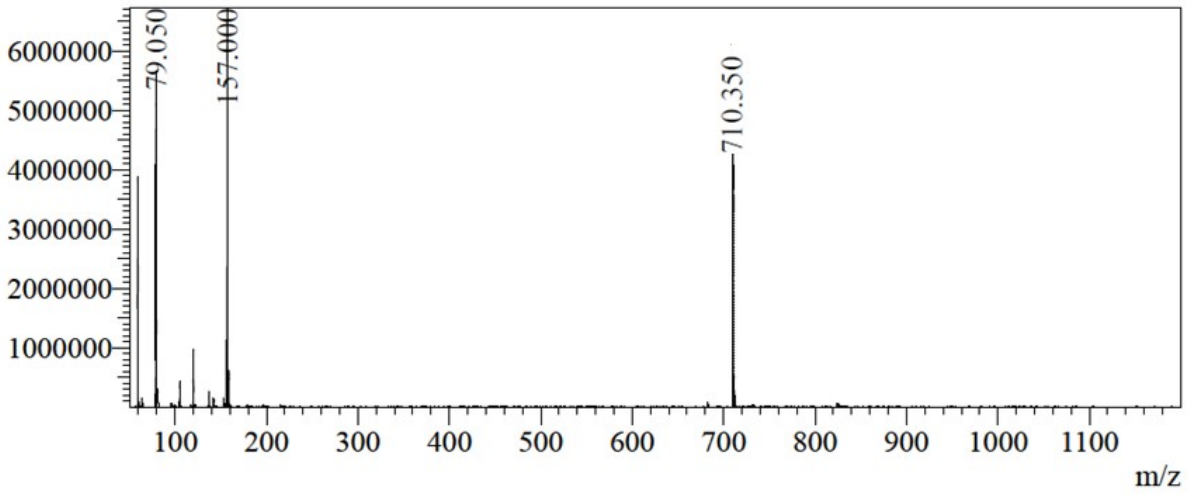

Figure S3. Mass spectrum of **BBS**

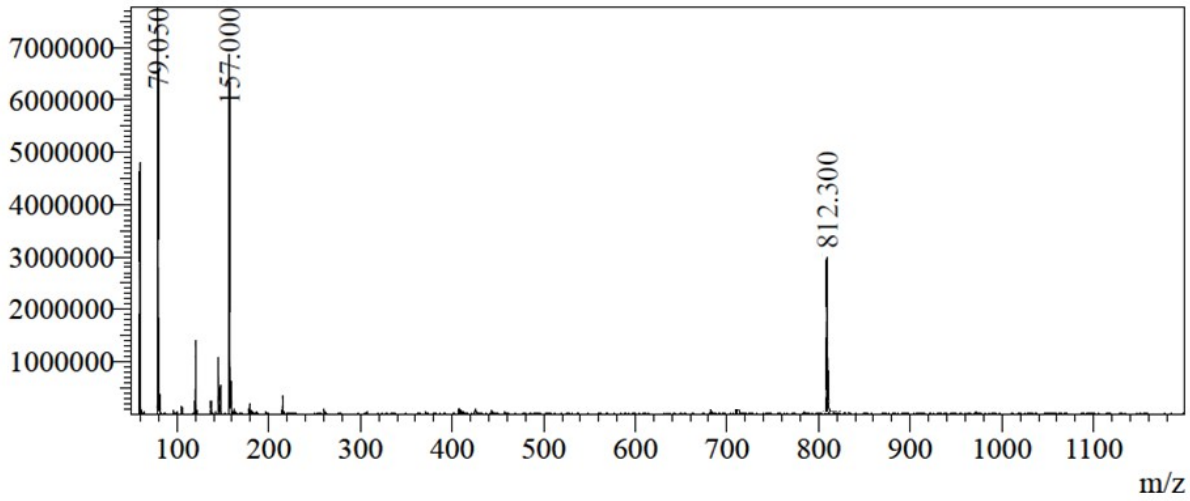

Figure S4. Mass spectrum of **BBS**+Cu^{2+} complex

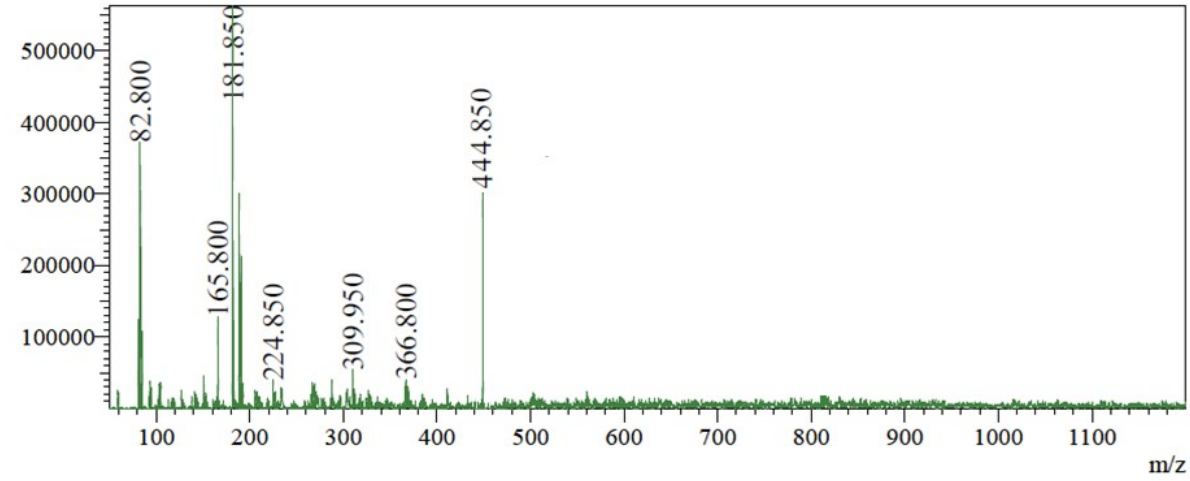

Figure S5. Mass spectrum of **BBS**+OCl^- complex

2.Calculation of the detection limit (DL):

The detection limit DL of **BBS** for Cu^{2+} was determined from the following equation:

DL = K* Sb1/S

Where K = 2 or 3 (we take 3 in this case); Sb1 is the standard deviation of the blank solution; S is the slope of the calibration curve.

From the graph Fig.S6, we get slope = 255.72, and Sb1 value is 222.782.

Thus, using the formula we get the Detection Limit for Cu^{2+} = 2.61 μM.

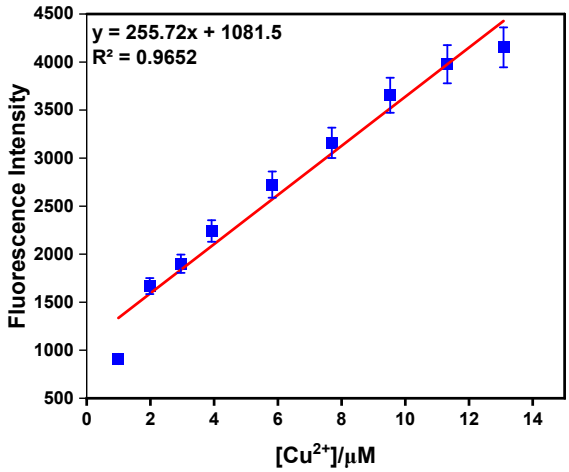

Figure S6. Changes of fluorescence intensity of **BBS** as a function of [Cu^{2+}] at 585 nm.

The detection limit DL of **BBS** for OCl^- was determined from the following equation:

DL = K* Sb1/S

Where K = 2 or 3 (we take 3 in this case); Sb1 is the standard deviation of the blank solution; S is the slope of the calibration curve.

From the graph Fig.S7, we get slope = 149.48, and Sb1 value is 97.76796.

Thus, using the formula we get the Detection Limit for OCl^- = 1.96 μM.

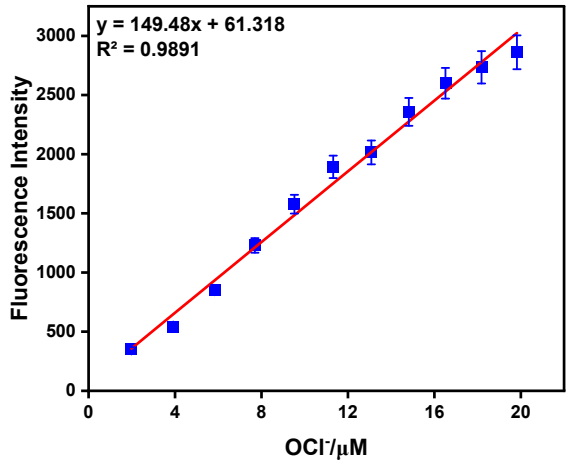

Figure S7. Changes of Fluorescence Intensity of **BBS** as a function of [OCl^-] at 575 nm.

The detection limit DL of **BBS** for OCl^- in tap water was determined from the following equation:

DL = K* Sb1/S

Where K = 2 or 3 (we take 3 in this case); Sb1 is the standard deviation of the blank solution; S is the slope of the calibration curve.

From the graph Fig.S8, we get slope = 4.304, and Sb1 value is 3.192.

Thus, using the formula we get the Detection Limit for OCl^- = 2.22 μM.

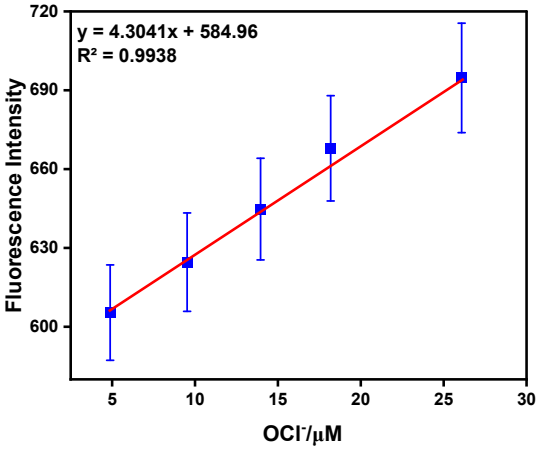

Figure S8. Changes of fluorescence Intensity of **BBS** as a function of [OCl^-] in tap water at 575 nm.

The detection limit (DL) of **BBS** -Cu^{2+} complex with DNA and BSA was determined from the following equation:

DL = K* Sb1/S

Where K = 2 or 3 (we take 3 in this case); Sb1 is the standard deviation of the blank solution; S is the slope of the calibration curve.

From UV-*vis* (a) and fluorescence titration (b) of **BBS** -Cu^{2+} complex with DNA (Fig.S9), slope values are -0.0103, -5.4204, and Sb1 values as 0.194, 71.911 respectively.

From UV-*vis* (c) and fluorescence titration (d) of **BBS** -Cu^{2+} complex with BSA (Fig.S9), slope values are -0.4464, -2713.8 and Sb1 values are 0.01, 29.564 respectively.

Thus, using the formula we have calculated the detection limit for **BBS** -Cu^{2+} complex with DNA from UV-*vis* and fluorescence titration 58.35 μM and 39.95 μM respectively. And **BBS** -Cu^{2+} complex with BSA from UV-*vis* and fluorescence titration 0.041 μM and 0.032 μM respectively.

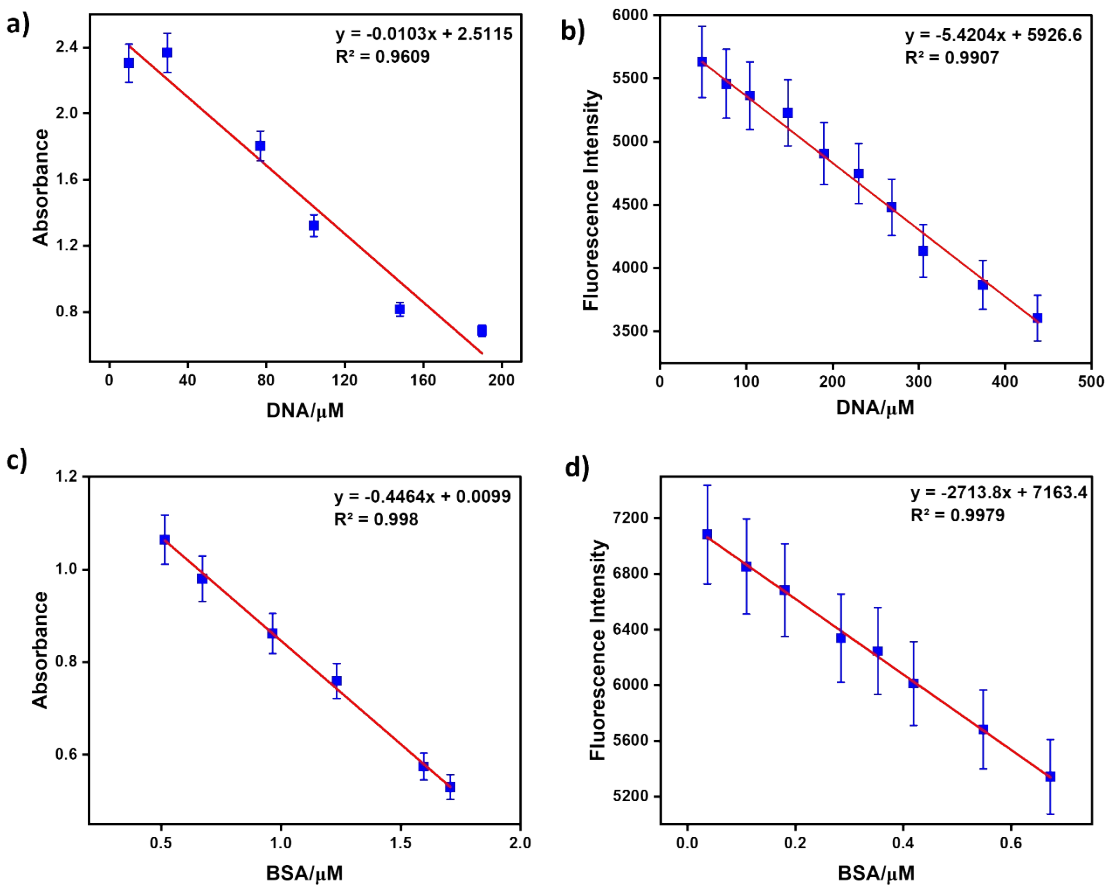

Figure S9. Changes of absorbance at 552 nm (a) and emission at 585 nm (b) of **BBS** -Cu^{2+} complex (c = 2.0 × 10^{-5} M) upon addition of ct DNA (c = 2 mM in base pairs). Changes of absorbance at 552 nm (c) and emission at 585 nm (d) of **BBS** -Cu^{2+} complex (c = 2.0 × 10^{-5} M) upon addition of BSA (c = 7.4 μM).

3.Jobs plot analysis:

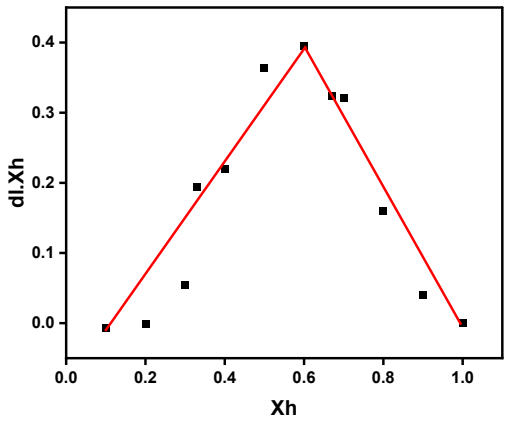

Figure S10. Job's plot diagram of receptor **BBS** for Cu^{2+} (where Xh is the mole fraction of host **BBS** and ΔI indicates the change of the intensity).

4. Binding constant determination:

The binding constant value of cation Cu^{2+} with the sensor has been determined from the emission intensity data following the modified Benesi–Hildebrand equation, $1/\Delta I = 1/\Delta I$ max + $(1/K[C])(1/\Delta I$ max). Here ΔI = I-Imin and ΔI max = Imax-Imin, where Imin, I, and Imax are the emission intensities of sensor considered in the absence of guest, at an intermediate concentration and at a concentration of complete saturation of guest where K is the binding constant and [C] is the guest concentration respectively. From the plot of (Imax-Imin)/(I-Imin) against $[C]^{-1}$ for sensor, the value of K has been determined from the slope. The association constant (K_a) as determined by fluorescence titration method for sensor with Cu^{2+} is found to be 1 x 10^4 M^{-1} (error < 10%).

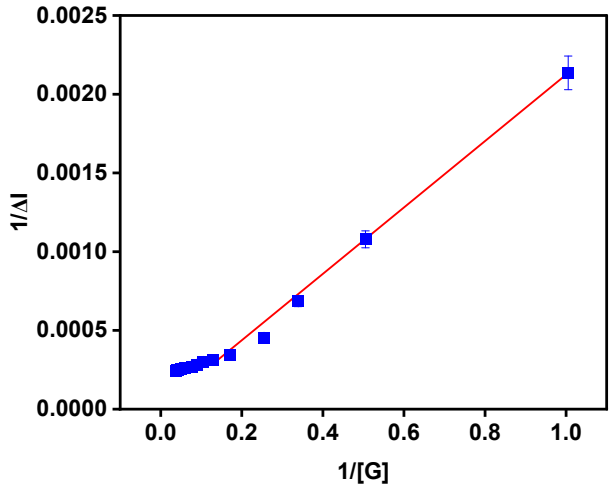

Figure S11. Benesi–Hildebrand plot from fluorescence titration data of receptor (20μM) with Cu^{2+} [G].

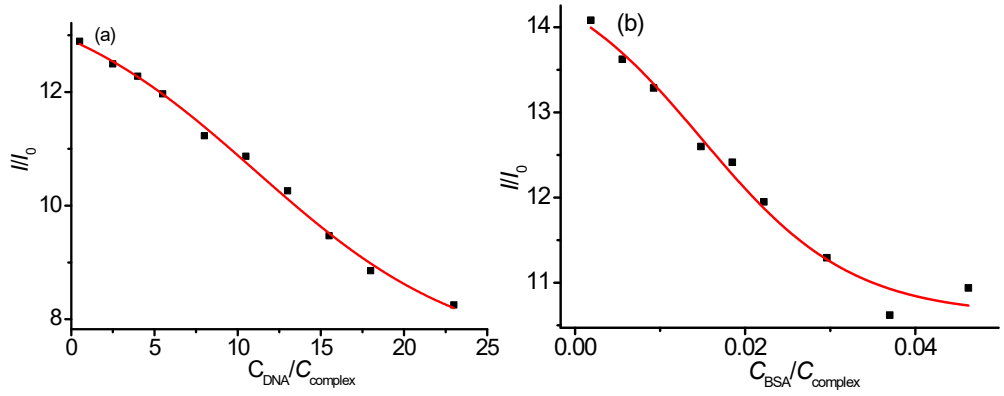

Figure S12. Non-linear fitting curves of binding isotherms resulting from spectrofluorometric titrations of **BBS**+ Cu^{2+} complex for the determination of binding constants (K_b) with ct DNA (a) and BSA(b). Red lines represent the best fits to the theoretical model.

The binding constants of **BBS** (Lig) with Cu^{2+} and **BBS**+Cu^{2+} complex with ct DNA and BSA were determined from the fluorometric titration spectra by non-linear fitting of the experimental data to the theoretical model in the following equation:[1]

$$\frac{I}{I_0} = 1 + \frac{Q-1}{2}\left(A + xn + 1 - \sqrt{(Q + xn + 1)^2 - 4xn}\right) \quad \text{(Equation 1)}$$

where $Q = I/I_0$ is the minimal emission intensity in the presence of excess ligand; n is the number of independent binding sites.

$A = 1/(K_b \times C_{\text{Lig or complex}})$;

$x = C_{Cu^{2+}\text{or DNA or BSA}}/C_{\text{Lig or complex}}$ is the titration variable

5. Rate constant calculation

The changes of emission curve of BBS (c =2x10^{-5}M) at different time interval by addition of Cu^{2+} and OCl^- (c =2x10^{-4}) and calculation of first order rate constant:

Fig.S13 represents the changes of emission intensity at different time interval by addition of Cu^{2+}. From the time vs. fluorescent intensity plot of **BBS** + Cu^{2+} at fixed wavelength at 585 nm by using first order rate equation we get the rate constant K= slope x 2.303 = 81.098 x 2.303 = 186.7 Sec^{-1}

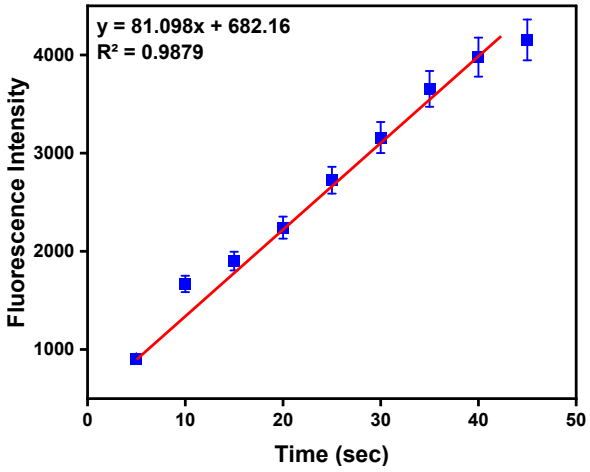

Figure S13. The first order rate equation by using Time vs. fluorescent intensity plot at 585nm.

Fig.S14 represents the changes of emission intensity at different time interval by addition of OCl^-. From the time vs. fluorescent intensity plot of **BBS**+ OCl^- at fixed wavelength at 574 nm by using first order rate equation we get the rate constant K= slope x 2.303 = 53.195 x 2.303 = 122.5 Sec^{-1}.

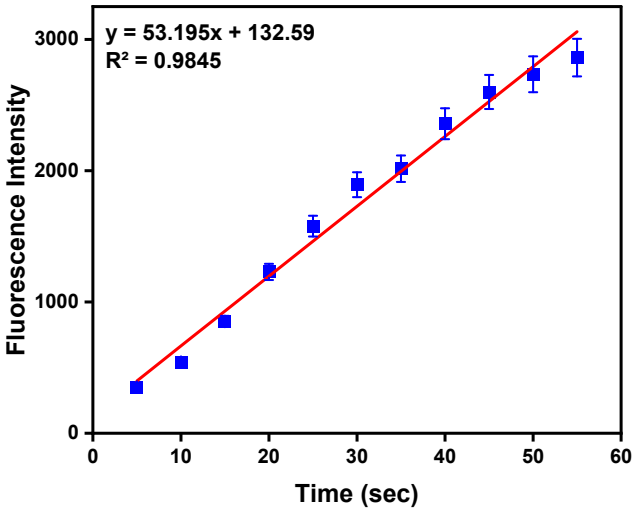

Figure S14. The first order rate equation by using Time vs. fluorescent intensity plot at 574 nm.

Fig.S15 represents the changes of emission intensity at different time interval by addition of DNA and BSA in **BBS** + Cu^{2+} solution. From the time vs. fluorescent intensity plot of **BBS** + Cu^{2+} in presence of DNA and BSA at fixed wavelength at 585 nm by using first order rate equation we get the rate constant K = slope × 2.303 as 105.82 Sec^{-1} and 110.55 Sec^{-1} respectively.

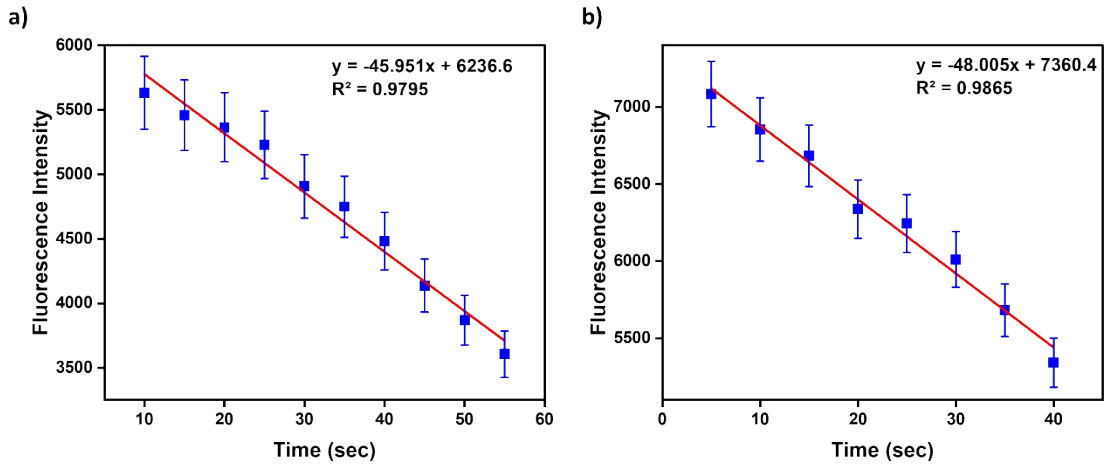

Figure S15. The first order rate equation for a) DNA an b) BSA by using Time vs. fluorescent intensity plot at 585 nm.

6. **Water analysis:**

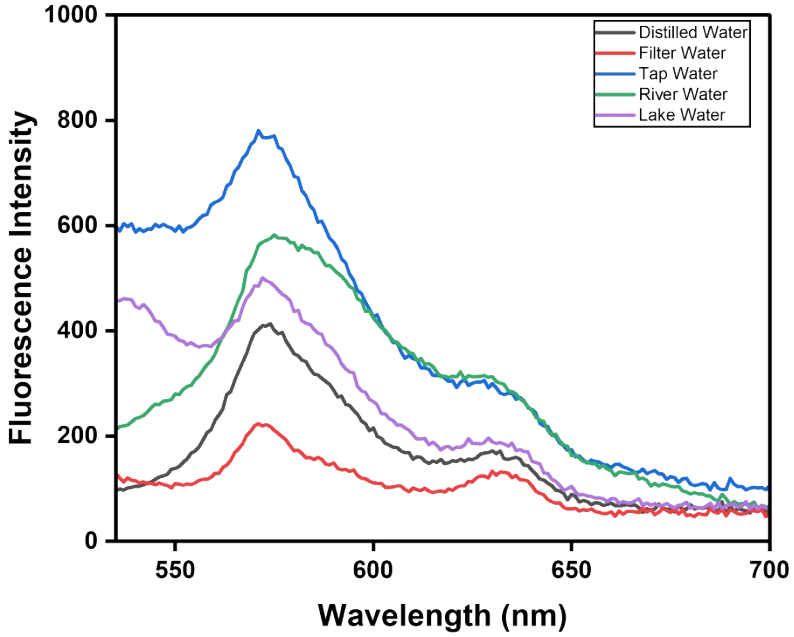

Figure S16. Changes in emission intensity of **BBS** (c = 2×10^{-5}M) on binding with OCl^- in various water samples.

7. **pH Study:**

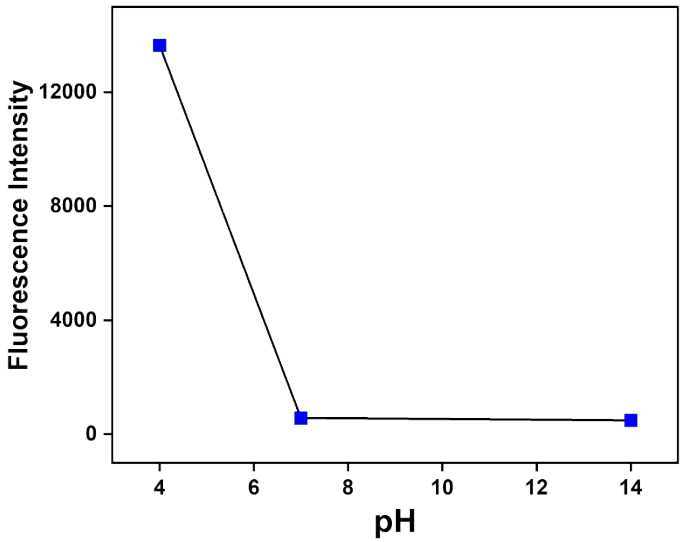

Figure S16. Changes in emission intensity of **BBS** (c = 2×10^{-5}M) at different pH concentrations.

8. Computational details:

Density Functional Theory (DFT)[2] calculations were conducted using the Gaussian 09 (Revision A.02) package, with "Gauss View" utilized for visualizing molecular orbitals. Becke's three-parameter hybrid-exchange functional, the Lee-Yang-Parr expression for nonlocal correlation, and the Vosko-Wilk-Nuair 1980 local correlation functional (B3LYP) were employed in the calculation.[3] Optimization of **BBS** and single-point energy calculations in the gas phase were performed using the 6-31+(g) basis set. The Lanl2dz basis set was used for Cu^{2+} and for H atoms we used 6-31+(g) basis set; for C, N, O, Cu atoms we employed LanL2DZ as basis set for all the calculations. The calculated electron-density plots for frontier molecular orbitals were prepared by using Gauss View 5.1 software. All the calculations were performed with the Gaussian 09W software package.[4]

9. In vitro cytotoxicity test:

A trypan blue cytotoxicity assay was performed on goat blood lymphocytes to determine the LD50 (lethal dose 50) of **BBS**. Lymphocytes were isolated using density gradient centrifugation[5] and incubated with **BBS** concentrations (5, 10, and 20 μM) for 2 hours at room temperature. Cells were then stained with 0.1% trypan blue[6] for 8-10 minutes, and non-viable cell counts were performed under a 10X light microscope. A linear equation was constructed, yielding an LD50 value of 12.71 μM, indicating relatively low toxicity. This assay, based on membrane integrity, confirmed **BBS's** safety profile, making it a promising probe for further investigation.

10. References:

1. F. H. Stootman, D. M. Fisher, A. Rodger, J. R. Aldrich-Wright, Analyst., 131 (2006) 1145.
2. R. G. Parr and W. Yang, *Density Functional Theory of Atoms and Molecules*, Oxford University Press, Oxford, 1989.
3. (a) A. D. Becke, *J. Chem. Phys.,* 98 **(**1993) 5648. (b) C. Lee , W. Yang and R. G. Parr, *Phys. Rev. B*, 37 (1998) 785.
4. M. J. Frisch, G. W. Trucks, H. B. Schlegel, G. E. Scuseria, M. A. Robb, J. R. Cheeseman, G. Scalmani, V. Barone, B. Mennucci, G. A. Petersson, H. Nakatsuji, M. Caricato, X. Li, H. P. Hratchian, A. F. Izmaylov, J. Bloino, G. Zheng, J. L. Sonnenberg, M. Hada, M. Ehara, K. Toyota, R. Fukuda, J. Hasegawa, M. Ishida, T. Nakajima, Y. Honda, O. Kitao, H. Nakai, T. Vreven, J. A. Montgomery Jr., J. E. Peralta, F. Ogliaro, M. Bearpark, J. J. Heyd, E. Brothers, K. N. Kudin, V. N. Staroverov, R. Kobayashi, J. Normand, K. Raghavachari, A. Rendell, J. C. Burant, S. S. Iyengar, J. Tomasi, M. Cossi, N. Rega, J. M. Millam, M. Klene, J. E. Knox, J. B. Cross, V. Bakken, C. Adamo, J. Jaramillo, R. Gomperts, R. E. Stratmann, O. Yazyev, A. J. Austin, R. Cammi, C. Pomelli, J. W. Ochterski, R. L. Martin, K. Morokuma, V. G. Zakrzewski, G. A. Voth, P. Salvador, J. J. Dannenberg, S. Dapprich, A. D. Daniels, Ö. Farkas, J. B. Foresman, J. V Ortiz, J. Cioslowski and D. J. Fox, Gaussian Inc., 2009, Wallingford CT.
5. A. Böyum, (1968). Isolation of mononuclear cells and granulocytes from human blood. Isolation of monuclear cells by one centrifugation, and of granulocytes by combining centrifugation and sedimentation at 1 g. Scandinavian journal of clinical and laboratory investigation. Supplementum, 97, 77-89.
6. J. Fassy, K. Tsalkitzi, M. Goncalves-Maia, & V. M. Braud, (2017). Current protocols in immunology.